



## PSHA input model documentation for Indian Ocean (OIN)

GEM Hazard Team

## Version history

Table 1 summarises version history for the OIN input model, named according to the versioning system described [here](#), and indicating which version was used in each of the global maps produced since 2018. Refer to the [GEM Products Page](#) for information on which model versions are available for various use cases. The changelog describes the changes between consecutive versions and are additive for all versions with the same model year.

**Table 1** – *Version history for the OIN input model.*

<b>Version</b>	<b>2018.1</b>	<b>2019.1</b>	<b>2022.1</b>	<b>2023.1</b>	<b>Changelog</b>
v2024.0.0					First version of the model created in FORCE

The following text describes v2024.0.0.

**Authors:** K. Bayliss, C. Brooks, R. Styron, M. Pagani.

## 1 Summary

The hazard model for the Indian Ocean covers the region from the Central Indian ridge to the Macquarie Ridge south of New Zealand. It covers the islands of the Maldives, Chagos islands, the Australian external territories of Cocos and Christmas islands, and Rodrigues island (Mascarene Islands). This model, and the associated models for the Atlantic and Pacific oceans, were developed as part of the Forecasting and Communicating Earthquake Risk (FORCE) project, supported by USAID Bureau for Humanitarian Assistance (BHA). The model was built for the [OpenQuake \(OQ\) engine](#) by the GEM secretariat.

## 2 Tectonic overview

The Eastern and Western (Indo-Australian) sections of the Indian plate are separated by the Carlsberg and Central Indian ridges, with the Rodriguez Triple Junction at the boundary with the Antarctic plate in the South. The section of the Indian Ocean plate West of the Central Indian ridge is included in the Atlantic ocean model (OAT), with this model focusing instead on the Western extent and extending as far East as the Macquarie ridge south of New Zealand. This model does not include the Sumatra subduction zone to the East, but this area has played host to some of the largest oceanic earthquakes not associated with subduction, including the November 2012  $M_w$  8.3 and  $M_w$  8.6 events at the Eastern extent of the Indo-Australian ridge and the 1983  $M_w$  7.7 event near the Chagos islands at the Western extent, one of the largest recorded normal fault events. Seismicity along the theorised Indo-Australian ridge seems to be primarily associated with the eastern and western extents, with very little observed seismicity extending to the portion south of the Maldives. This model thus primarily consists of large zones describing oceanic crust, with varying degrees of observed seismicity, and (generally slow) mid-ocean spreading ridges at the boundaries.

The Indo-Australian plate itself is most likely separated into smaller plates with diffuse boundaries (*Wiens et al, 1985*), but several different theories exist on where these boundaries lie, and the recorded seismicity captured in global catalogues does not provide many answers. This region also contains the North-South trending Ninety-East ridge, a feature that is quite prominent on bathymetric studies but does not seem to correlate particularly clearly with recent observed seismicity.

The most active oceanic zone in the OIN model covers the Cocos and Christmas islands (Australian external territories), while the Maldives and Lakshadweep (India) islands lie in a zone of very low observed seismicity. The Chagos islands lie in a suspected triple junction between the Indian Ocean ridge and the Indo-Australian ridge. The Indian ocean model also includes one island from the Mascarene islands (Île Rodrigues, Mauritius) which lies in an oceanic spreading zone to the North-West of a triple junction with the Indian-Antarctic ridge.

### 3 Basic Datasets

This model uses the magnitude-homogenised GEM 2024 global homogenised catalogue. This catalogue merged the [ISCGEM v10](#) catalogue (*International Seismological Centre, 2025; Storchak et al., 2013, 2015; Di Giacomo et al., 2018*), the [Global CMT catalogue](#) (*Dziiewonski et al., 1981; Ekström et al., 2012*) and the [comcat/ANSS](#) (*USGS, 2017*) catalogue and includes events from 1900 - 2020, homogenised to  $M_W$ .

We also use Global Centroid Moment Tensor (GCMT) focal mechanisms from 1976-2020 (*Dziiewonski et al., 1981; Ekström et al., 2012*).

### 4 Hazard Model

#### 4.1 Seismic Source Characterisation

The seismic source model for this region currently uses only distributed active shallow seismicity modeled as a grid of **point sources**.

We model distributed seismicity with an approach that combines area sources with smoothed seismicity, incorporating methods from *Frankel (1995)* and *Helmstetter et al. (2007)*, with the [source zone approach commonly used to build GEM models](#). We build a source model for the crustal subcatalogue encompassed by each source zone polygon, with occurrence rates at a bin spacing of  $M=0.1$ .

First, the completeness of the catalogues is established using an automated procedure that identifies optimal windows from the catalogue. Then the catalogue is declustered to remove and the Magnitude-Frequency (MFD) parameters are calculated for each zone. We compute the smoothed seismicity for a grid defined by h3 hexagons spanning the source polygon. The total rates expected from the MFD are then distributed according to the smoothed density, to create a spatially-varying model of seismicity.

In this model, epistemic uncertainty is considered in the distributed sources by including two types of declustering (*Uhrhammer, 1986* and *Zaliapin and Ben-Zion 2013*), each with a 0.5 weight in the logic tree. This choice of alternative declustering also provides alternative MFD parameters. Further, two smoothing approaches were used, with the adaptive smoothing approach of *Helmstetter (2007)* weighted 0.7 and the fixed kernel smoothing with 3 fixed kernels weighted at 0.3. Source zone characteristics are described for both declustering approaches in [Table 2](#), and the sources are shown in [Figure 1](#)

#### 4.2 Ground Motion Characterisation

The ground motion characterisation used available records for all oceanic events to derive a single GMC for all oceans models. Spreading and transform share one ground motion logic tree, with the GMC derived using (limited) ground-motion records for mid-ocean regions (mostly from Iceland) and following the choices of the ESHM20 model for Iceland (*Danciu*

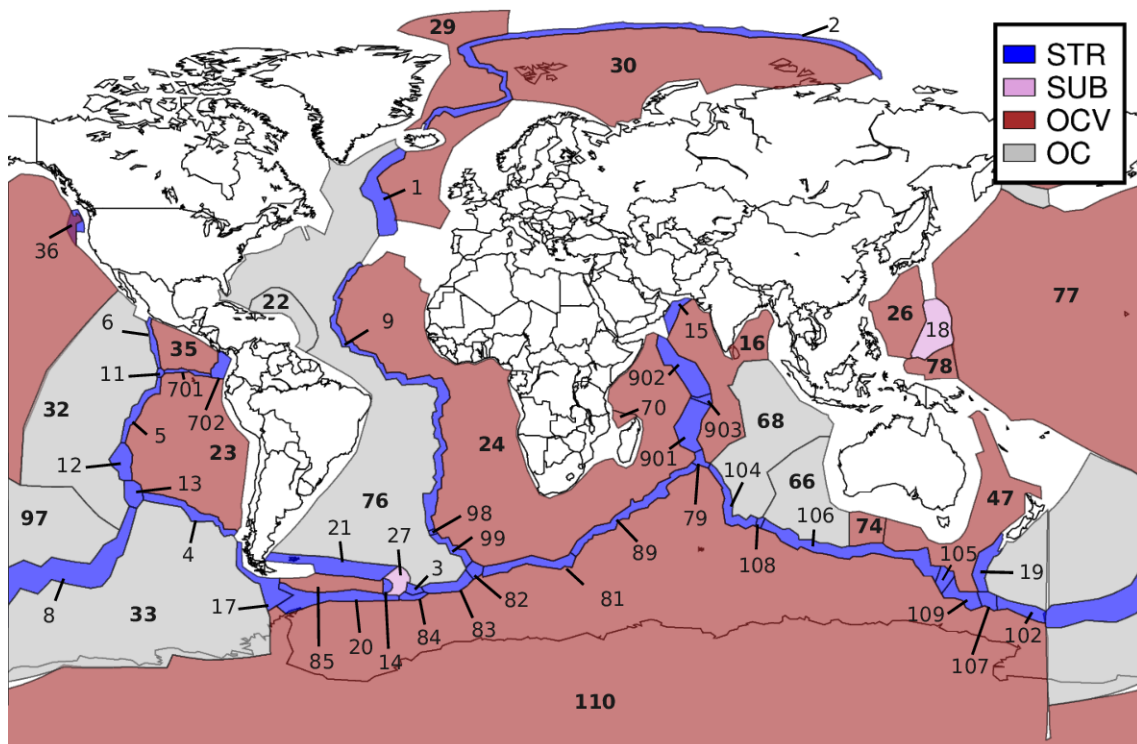


**Figure 1** – Ocean model sources with ground motion regions. STR - Spreading and Transforms; SUB - Subduction; OCV - Oceanic Crust with Volcanism; OC - Oceanic Crust (no volcanism).

<b>SZ</b>	<b>a-Value UH</b>	<b>b- Value UH</b>	<b>a-Value ZBZ</b>	<b>b- Value ZBZ</b>	$M_{max,obs}$	<b>Description</b>
16	4.299	1.0	2.677	0.7	7.38	quiet oceanic crust around India, covers Maldives
68	5.414	0.97	5.687	1.018	8.19	active oceanic zone West of Indonesia covering Indo-Australian rift and possible Capricorn ridge
66	4.055	1.0	2.42	0.7	7.39	active ocean zone covering region SW of Australia
74	3.952	0.88	3.952	0.878	7.08	low seismicity oceanic zone South of Australia
47	3.067	0.748	3.067	0.748	7.16	low seismicity oceanic zone South-East of Australia
15	4.596	1.0	5.101	1.1	5.91	Indian-Arabian fracture zone (transform)
79	7.565	1.4	7.565	1.4	6.10	Mid-Indian ridge triple junction with Antarctic ridge
80	7.582	1.312	7.885	1.376	8.02	East-West trending spreading ridge South of Madagascar
104	7.653	1.372	7.634	1.37	6.61	Indian-Antarctic ridge from triple junction East
105	4.283	0.789	4.232	0.781	6.88	hypothesised triple junction between Antarctic and Tasman fracture zone
106	6.942	1.19	6.960	1.192	6.67	Eastern Southern Indian ocean spreading ridge
107	7.606	1.475	7.487	1.465	6.02	Indian-Pacific-Antarctic fracture zone Triple Junction
108	5.351	1.1	6.084	1.236	5.93	Eastern Southern Indian ocean spreading ridge, possible triple junction with Capricorn ridge
109	4.201	0.707	4.077	0.687	6.83	Eastern Southern Indian Ocean spreading ridge
902	8.209	1.446	8.37	1.478	7.57	Northern mid-Indian ridge
903	7.116	1.495	7.206	1.45	7.70	African-Indian ridge meets Indo-Australian rift triple junction, Chagos islands
901	8.328	1.482	7.922	1.428	6.64	Mid-Indian ridge South, includes Rodrigues (Mascarene Islands)

**Table 2** – Crustal source zone parameters and descriptions.

*et al.*, 2021). For oceanic crust, two different logic trees are used depending on whether or not the zone is expected to include volcanism, with this classification coming from the presence or absence of volcanoes in the Smithsonian Global Volcanism Project (2003). The

classification of each zone is shown in Figure 1. The GMMs for each source type are shown in Table 3

<b>Spreading and Transforms</b>	<b>Weight</b>
ChiouYoungs2014	0.5
ESHM20 ASCR Backbone (Iceland)	0.5
<b>Oceanic Crust (Volcanism)</b>	<b>Weight</b>
Atkinson2010Hawaii	0.2
ASK14 JPN	0.2
BSSA14 low Q	0.2
CB14	0.2
CY14 JPN	0.2
<b>Oceanic Crust (No volcanism)</b>	<b>Weight</b>
ASK14	0.25
BSSA14	0.25
CB14	0.25
CY14	0.25

**Table 3** – GMPes used in the OIN model.

## 5 Results

Hazard curves were computed with the [OQ engine](#) for the following:

- Intensity measure types (IMTs): peak ground acceleration (PGA) and spectral acceleration (SA) at 0.2s, 0.3s, 0.6s, 1.0s, and 2s
- reference site conditions with shear wave velocity in the upper 30 meters (Vs30) of 760-800 m/s, as well as for Vs30 derived from a topography proxy (Allen and Wald, 2009)

Hazard maps were generated for each reference site condition-IMT pair for 10% and 2% probabilities of exceedance (POEs) in 50 yrs. Additionally, disaggregation by magnitude, distance, and epsilon was computed for the following cities: Male, Diego Garcia, Pulu Selma. The results were produced as csv files and bar plots for each of the following combinations:

- hazard levels for 10% and 2% POE in 50 yrs
- PGA and SA at 0.2s, 0.3s, 0.6s, and 1.0s
- Vs30=800 m/s

All calculations used a ground motion sigma truncation of 5. Results were computed for sites with 6 km spacing

Visit the [GEM Interactive Viewer](#) to explore the Global Seismic Hazard Map values (PGA for  $V_s30=800$  m/s, 10% poe in 50 years). For a comprehensive set of hazard and risk results, see the [GEM Products Page](#).

## 6 References

Allen, T. I., and Wald, D. J., 2009, On the use of high-resolution topographic data as a proxy for seismic site conditions  $V_s30$ , *Bulletin of the Seismological Society of America*, 99, no. 2A, 935-943

Danciu, L., Nandan, S., Reyes, C., Basili, R., Weatherill, G., Beauval, C., Rovida, A., Vilanova, S., Sesetyan, K., and Bard, P.-Y. (2021). The 2020 update of the european seismic hazard model: Model overview. Technical Report 001, v1.0.0, EFEHR

Dziewonski, A. M., T.-A. Chou and J. H. Woodhouse, Determination of earthquake source parameters from waveform data for studies of global and regional seismicity, *J. Geophys. Res.*, 86, 2825-2852, 1981. doi:10.1029/JB086iB04p02825

Ekström, G., M. Nettles, and A. M. Dziewonski, The global CMT project 2004-2010: Centroid-moment tensors for 13,017 earthquakes, *Phys. Earth Planet. Inter.*, 200-201, 1-9, 2012. doi:10.1016/j.pepi.2012.04.002

Frankel, A. (1995). Mapping seismic hazard in the central and eastern United States. *Seismological Research Letters*, 66(4), 8-21.

Di Giacomo, D., E.R. Engdahl and D.A. Storchak (2018). The ISC-GEM Earthquake Catalogue (1904–2014): status after the Extension Project, *Earth Syst. Sci. Data*, 10, 1877-1899, doi: 10.5194/essd-10-1877-2018.

Helmstetter, A., Y.Y. Kagan, and D.D. Jackson. High-resolution Time-independent Grid-based Forecast for  $M \geq 5$  Earthquakes in California. *Seismological Research Letters*, 2007, 78 (1), pp.78-86.

International Seismological Centre (2025), ISC-GEM Earthquake Catalogue, <https://doi.org/10.31905/d808b825>

Smithsonian Institution. (2003). Global Volcanism Program. American Geological Institute. Geological Survey (U.S.). Environmental Systems Research Institute (Redlands, Calif.). Global GIS : volcanoes of the world ; volcano basic data. [Shapefile]. American Geological Institute. Retrieved from <https://maps.princeton.edu/catalog/harvard-glb-volc>

Storchak, D.A., D. Di Giacomo, I. Bondár, E.R. Engdahl, J. Harris, W.H.K. Lee, A. Villaseñor and P. Bormann (2013). Public Release of the ISC-GEM Global Instrumental Earthquake Catalogue (1900-2009). *Seism. Res. Lett.*, 84, 5, 810-815, doi: 10.1785/0220130034.

Storchak, D.A., D. Di Giacomo, E.R. Engdahl, J. Harris, I. Bondár, W.H.K. Lee, P. Bormann and A. Villaseñor (2015). The ISC-GEM Global Instrumental Earthquake Catalogue (1900-2009):

Introduction, *Phys. Earth Planet. Int.*, 239, 48-63, doi: 10.1016/j.pepi.2014.06.009.

Uhrhammer, R. (1986). Characteristics of Northern and Central California Seismicity, *Earthquake Notes*, 57(1): 21

U.S. Geological Survey, Earthquake Hazards Program, 2017, Advanced National Seismic System (ANSS) Comprehensive Catalog of Earthquake Events and Products: Various, <https://doi.org/10.5066/F7MS3QZH>.

Wiens, D. A., DeMets, C., Gordon, R. G., Stein, S., Argus, D., Engeln, J. F., Lundgren, P., Quible, D., Stein, C., Weinstein, S., and Woods, D. F. (1985). A diffuse plate boundary model for Indian Ocean tectonics. *Geophysical Research Letters*, 12(7), 429-432

Zaliapin, I., and Ben-Zion, Y. (2013). Earthquake clusters in southern California I: Identification and stability. *Journal of Geophysical Research: Solid Earth*, 118(6), 2847-2864.

Last processed: Friday 11<sup>th</sup> April, 2025 @ 16:52

[www.globalquakemodel.org](http://www.globalquakemodel.org)

If you have any questions please contact the GEM Foundation Hazard Team at: [hazard@globalquakemodel.org](mailto:hazard@globalquakemodel.org)